

RESEARCH ARTICLE | JANUARY 03 2023

Diameter-dependent ultrafast lithium-ion transport in carbon nanotubes

Zhong-Heng Fu; Xiang Chen ; Nan Yao; ... et. al



J. Chem. Phys. 158, 014702 (2023)
<https://doi.org/10.1063/5.0131408>



View
Online



Export
Citation

CrossMark

Articles You May Be Interested In

Engineering interface upgrade of $\text{LiNi}_{0.8}\text{Co}_{0.1}\text{Mn}_{0.1}\text{O}_2$ cells from $\text{PYR}_{1(4\text{CN})}(2\text{O}_2)\text{TFSI}$ with cyano and ether groups as dual functional pyrrolidine electrolyte

Appl. Phys. Lett. (February 2023)

Development of bulk-type all-solid-state lithium-sulfur battery using LiBH_4 electrolyte

Appl. Phys. Lett. (August 2014)

Research Update: Ca doping effect on the Li-ion conductivity in NASICON-type solid electrolyte
 $\text{LiZr}_2(\text{PO}_4)_3$: A first-principles molecular dynamics study

APL Mater. (June 2018)



Time to get excited.
Lock-in Amplifiers – from DC to 8.5 GHz



Find out more



Zurich
Instruments

Diameter-dependent ultrafast lithium-ion transport in carbon nanotubes

Cite as: J. Chem. Phys. 158, 014702 (2023); doi: 10.1063/5.0131408

Submitted: 20 October 2022 • Accepted: 7 December 2022 •

Published Online: 3 January 2023



View Online



Export Citation



CrossMark

Zhong-Heng Fu,¹ Xiang Chen,^{1,a)} Nan Yao,¹ Le-Geng Yu,¹ Xin Shen,¹ Shaochen Shi,² Rui Zhang,^{3,4} Zhengju Sha,² Shuai Feng,⁵ Yu Xia,² and Qiang Zhang¹

AFFILIATIONS

¹ Beijing Key Laboratory of Green Chemical Reaction Engineering and Technology, Department of Chemical Engineering, Tsinghua University, Beijing 100084, China

² ByteDance, Inc., Zhonghang Plaza, No. 43, North 3rd Ring West Road, Haidian District, Beijing 100086, China

³ Advanced Research Institute for Multidisciplinary Science, Beijing Institute of Technology, Beijing 100081, China

⁴ School of Materials Science and Engineering, Beijing Institute of Technology, Beijing 100081, China

⁵ College of Chemistry and Chemical Engineering, Taishan University, Tai'an 271021, China

Note: This paper is part of the JCP Special Topic on Chemical Physics of Electrochemical Energy Materials.

a) Author to whom correspondence should be addressed: xiangchen@mail.tsinghua.edu.cn

ABSTRACT

Ion transport in solids is a key topic in solid-state ionics. It is critical but challenging to understand the relationship between material structures and ion transport. Nanochannels in crystals provide ion transport pathways, which are responsible for the fast ion transport in fast lithium (Li)-ion conductors. The controlled synthesis of carbon nanotubes (CNTs) provides a promising approach to artificially regulating nanochannels. Herein, the CNTs with a diameter of 5.5 Å are predicted to exhibit an ultralow Li-ion diffusion barrier of about 10 meV, much lower than those in routine solid electrolyte materials. Such a characteristic is attributed to the similar chemical environment of a Li ion during its diffusion based on atomic and electronic structure analyses. The concerted diffusion of Li ions ensures high ionic conductivities of CNTs. These results not only reveal the immense potential of CNTs for fast Li-ion transport but also provide a new understanding for rationally designing solid materials with high ionic conductivities.

Published under an exclusive license by AIP Publishing. <https://doi.org/10.1063/5.0131408>

I. INTRODUCTION

Ion transport in solids is a critical scientific concept in the field of solid-state ionics.¹ Ion-conducting solids are classified into mixed ion–electron conductors (MIECs) and fast ion conductors (FICs, also known as solid electrolytes, SEs) according to the electronic conductivities of materials. Both MIECs and FICs have been widely used in energy storage and conversion devices, e.g., solid oxide fuel cells and solid-state batteries (SSBs).^{2,3} Despite the achievement that many MIEC and FIC materials have been synthesized and reported, the discovery of these materials primarily depends on the experimental “trial and error” or serendipitous discoveries.^{4,5} The relationship between material structures and ion transport is still ambiguous, limiting the rational design of MIEC and FIC materials and the construction of high-performance energy storage and conversion devices.

Fast lithium (Li)-ion conductors (FLICs) with fast Li-ion transport have attracted increasing attention due to the rapid development of solid-state Li batteries. Their crystalline structures, e.g., garnets,⁶ NASICONs,⁷ perovskites,⁸ thio-LISICONs,⁹ Li argyrodites,¹⁰ Li borohydrides,¹¹ Li nitrides,¹² Li hydrides,¹³ and Li halides,¹⁴ were confirmed to be associated with ion transports by unsupervised clustering analysis.¹⁵ Nanochannels in crystals provide ion transport pathways. The ultrahigh ionic conductivity (12 mS cm^{-1}) of $\text{Li}_{10}\text{GeP}_2\text{S}_{12}$ (LGPS),⁹ comparable to those of commercial liquid electrolytes, is ascribed to the straight one-dimensional diffusion channel along the [001] direction.¹⁶ Consequently, rationally designing the nanochannels is a promising approach to enabling targeted transport properties in solids. For instance, porous metal–organic framework-688 (MOF-688) exhibits an ionic conductivity of 0.34 mS cm^{-1} at 20°C through artificially constructing nanochannels.¹⁷

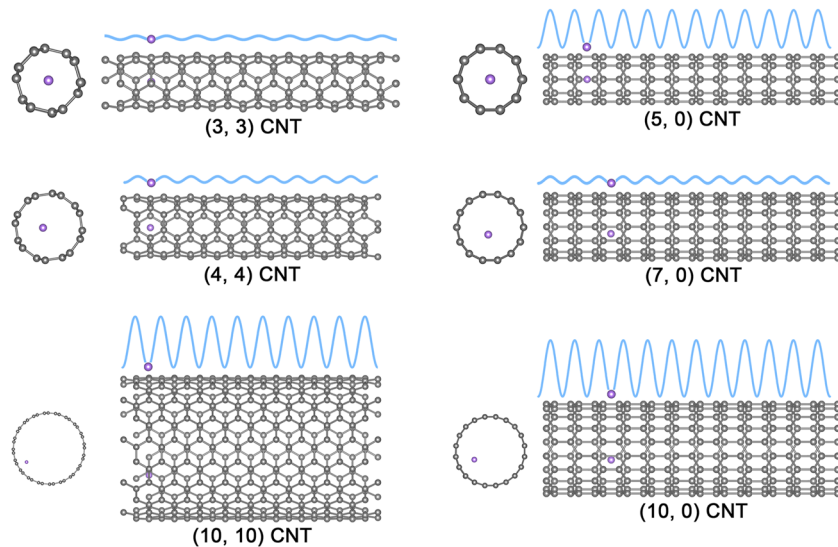


FIG. 1. Schematic of diameter-dependent Li transport in CNTs. The cyan curves represent the potential energy surfaces of Li ions. The C and Li atoms are marked gray and pink, respectively.

The controlled synthesis of single-chirality carbon nanotubes (CNTs) provides an unprecedented opportunity to sophisticatedly regulate nanochannels and subsequent ion transports by controlling the diameter and chirality.¹⁸ Diameter-dependent electrical conductivities shown by band gaps ranging from 0 to 0.08 eV have been achieved by the controlled synthesis.¹⁹ The interest in the transport of small molecules and ions in CNTs is initiated by the superfast water transport phenomenon.²⁰ A fivefold enhanced proton transport rate in the CNTs with a diameter of 1.6 nm was determined compared with that in bulk aqueous solutions.²¹ The Li-ion transport inside CNTs has been experimentally observed, along with an estimated ionic conductivity of 1 mS cm^{-1} .²² Parallel CNT arrays are practically applied to eliminate the void formation and Li dendrite growth at Li/SE interfaces in SSBs through fast Li-ion transport in CNTs.^{22,23} Although the fast Li-ion transport in CNTs has been elaborately observed through *in situ* high-resolution transmission electron microscopy,^{22,24} the transport mechanism remains elusive.

In this contribution, the Li-ion transport mechanism in CNTs is probed through first-principles calculations and *ab initio* molecular dynamics (AIMD) simulations (Fig. 1). A fast Li-ion transport with an ultralow activation energy of 10 meV is observed in both (4, 4) and (7, 0) CNTs with a diameter of 5.5 Å. The fast Li-ion transport in the (4, 4) and (7, 0) CNTs is attributed to the similar chemical environment of a Li ion during its transport, characterized by a constant Li-C bond length, electron transfer, and crystal orbital Hamilton population (COHP). The concerted diffusion of Li ions ensures high ionic conductivities of CNTs with high carrier concentrations. These results highlight the significance of understanding the chemical environment of a Li ion in rationally designing potential materials with high ionic conductivities.

II. METHODS

A. First-principles calculations

The first-principles calculations based on density functional theory (DFT) were performed by implementing Vienna *Ab initio*

Simulation Package (VASP).²⁵ The projector augmented wave (PAW) method was employed to describe the ion-electron interactions,²⁶ where valence electrons of Li and C are considered with $2s^1$ and $2s^22p^2$, respectively. Local density approximation (LDA) in the form of Ceperley–Alder was adopted for the exchange–correlation energy.²⁷ Note that the van der Waals (vdW) correction is not considered since the LDA already overestimates the binding interaction. The introduction of the vdW correction will result in a larger deviation.^{28,29} A kinetic energy cutoff of 520 eV was adopted for the plane wave expansion of the valence electron wave functions. Γ -centered Monkhorst–Pack k -points were sampled on a $1 \times 1 \times 5$ grid. The convergence criteria of $10^{-6} \text{ eV cell}^{-1}$ in energy and $10^{-2} \text{ eV } \text{\AA}^{-1}$ in force were adopted during structural optimizations. The lattice parameters of CNT models are summarized in Table S1. Armchair-type CNTs (3, 3), (4, 4), (5, 5), (6, 6), (7, 7), (8, 8), (9, 9), and (10, 10) CNTs with 36, 48, 60, 72, 84, 96, 108, and 120 atoms, respectively, and zigzag-type CNTs (5, 0), (6, 0), (7, 0), (8, 0), (9, 0), and (10, 0) CNTs with 60, 72, 84, 96, 108, and 120 atoms, respectively, were considered as model systems.

The climbing image nudged elastic band (CINEB) method was applied to search for the transition state (TS) and sample the energy profile of Li-ion diffusions in CNTs.³⁰ The Li-ion hopping between the hollow sites in the CNTs was investigated because of the stable adsorption of Li ions at the hollow sites.³¹ The detailed Li-ion diffusion pathway in armchair- and zigzag-type CNTs are shown in Fig. S1. A spiral diffusion path is observed in zigzag-type CNTs, compared to a straight diffusion mode along the tube axis in armchair-type CNTs. Eight intermediate images were used for each CINEB calculation. The spring constant between the images was set as $5.0 \text{ eV } \text{\AA}^{-2}$. Bader charge analyses were performed by the scripts of the Henkelman group.³² COHP analyses were performed employing the LOBSTER software.³³

B. *Ab initio* molecular dynamics simulations

AIMD simulations were performed employing VASP. A minimal Γ -centered $1 \times 1 \times 1$ grid was adopted for k -point sampling. Ten independent AIMD simulations were performed for the CNTs with

a preset carrier concentration, which are used for an averaged diffusivity and ionic conductivity. Multiple Li ions were randomly placed in the CNTs. The initial distances between Li ions were set above 2 Å to avoid unreasonable initial velocities in the simulation. Two C atoms were fixed in the AIMD simulation to avoid the artificial rotation of CNTs.

The procedure of the AIMD simulations is divided into three steps: (1) An annealing step from 100 to 300 K with a heating rate of 0.2 K fs⁻¹. (2) An equilibrium step using a canonical ensemble (*NVT*) with a Nose–Hoover thermostat^{34,35} for 2 ps. (3) A sampling step with the same thermostat for 10 ps to collect displacement events.

Diffusivity D was determined based on the random walk model,³⁶

$$D = \lim_{t \rightarrow \infty} \left[\frac{\langle [\vec{r}(t)]^2 \rangle}{2dt} \right], \quad (1)$$

where d is the diffusion dimensionality, t the time, and $\langle [\vec{r}(t)]^2 \rangle$ the averaged mean square displacement (MSD) over all Li atoms,

$$\langle [\vec{r}(t)]^2 \rangle = \frac{1}{N} \sum_{n=1}^N \langle [\vec{r}_n(t + t_0)]^2 - [\vec{r}_n(t_0)]^2 \rangle, \quad (2)$$

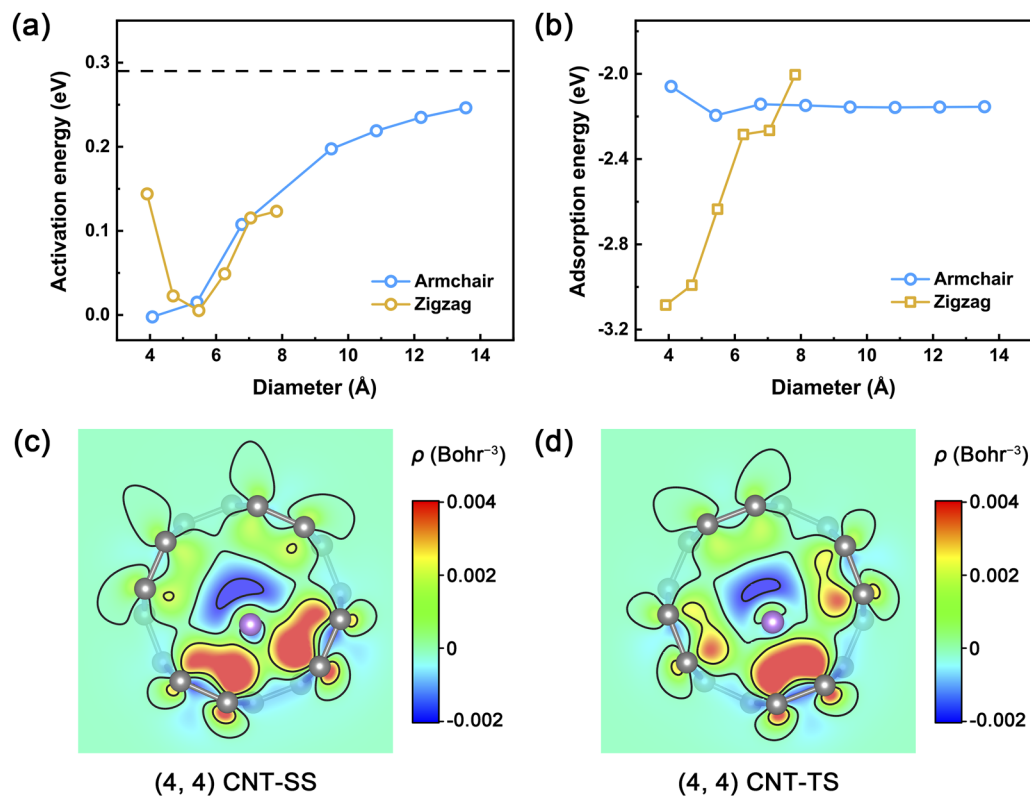


FIG. 2. The Li-ion diffusion in CNTs. (a) Activation energy and (b) Li-ion adsorption energy as a function of the diameter of CNTs. Charge density difference of the (4, 4) CNT involving a Li at (c) SS and (d) TS. The C and Li atoms are marked gray and pink, respectively. The red and blue regions denote charge accumulation and depletion, respectively.

where $\langle \vec{r}_n(t) \rangle$ is the displacement of the n^{th} Li atom at time t .

Ionic conductivity σ was calculated using the Nernst–Einstein equation,³⁷

$$\sigma = \frac{Z_c^2 e^2 C}{k_B T} D, \quad (3)$$

where Z_c , e , C , k_B , and T denote the valence state of carriers, electron charge, carrier concentration, Boltzmann constant, and temperature, respectively.

III. RESULTS AND DISCUSSION

A. Energetical analysis of Li-ion diffusion

The potential energy profiles of Li-ion diffusions in CNTs are shown in Fig. S2. The activation energies decrease first and then increase with increasing diameters for zigzag-type CNTs, compared with the monotonically increasing ones ranging from 2 to 246 meV for armchair-type CNTs [Fig. 2(a)]. The (5, 0), (8, 0), and (5, 5) CNTs exhibit activation energies of 149, 49, and 107 meV, respectively, in excellent agreement with previous theoretical reports (160,³⁸ 35,³⁹ and 79⁴⁰ meV). Similar activation energies of about 10 meV are observed in the metallic (4, 4) and semiconducting (7, 0) CNTs with

similar diameters of 5.5 Å despite different chiralities and electronic structures, ruling out the direct correlation between ion transport and electronic structures. The activation energy is much lower than those in routine SEs, e.g., LGPS (0.25 eV),⁹ garnet Li₇La₃Zr₂O₁₂ (0.31 eV),⁶ and Li_{1.3}Al_{0.3}Ti_{1.7}(PO₄)₃ (0.27 eV),¹⁶ suggesting flat potential energy surfaces of Li ions in CNTs (Fig. 1).

The interaction between Li and CNT is considered to illustrate the origin of the low activation energy. The Li-ion adsorption energy (E_{ad}) in CNTs is determined to evaluate the binding strength between Li and CNT,⁴¹

$$E_{\text{ad}} = E_{\text{CNT-Li}} - E_{\text{CNT}} - E_{\text{Li}}, \quad (4)$$

where $E_{\text{CNT-Li}}$, E_{CNT} , and E_{Li} are the total energies of CNT-Li, CNT, and a Li atom, respectively. The adsorption energy increases with the diameter for zigzag-type CNTs, contrary to the diameter-independent adsorption energy of \sim 2.15 eV for armchair-type CNTs [Fig. 2(b)]. The interaction between the Li ion and CNT is further evaluated by charge density difference, which is defined as follows:

$$\rho_{\text{diff}} = \rho_{\text{CNT-Li}} - \rho_{\text{CNT}} - \rho_{\text{Li}}, \quad (5)$$

where $\rho_{\text{CNT-Li}}$, ρ_{CNT} , and ρ_{Li} denote the charge density of CNT-Li, CNT, and a Li atom, respectively. The strong electron accumulation between the Li ion and the (4, 4)/(7, 0) CNT is observed at both the stable state (SS) and TS of Li diffusions [Figs. 2(c), 2(d), and S3], contributing to the binding between the Li and CNT.

B. Electronic origin of fast Li-ion diffusion

The Li-C bond length, Bader charge, and COHP analyses are performed to reveal the structural and electronic origin of the changed activation energy during Li diffusion. The Li-C bond lengths in both armchair- and zigzag-type CNTs decrease with increasing diameters except for the (3, 3) and (5, 0) CNTs (Fig. S4), in which the Li-C bonds are confined due to their small diameters of 4.1 and 3.9 Å, respectively. The differences between the Li-C bond lengths at SS and TS become increasingly negative with increasing diameters of the armchair- and zigzag-type CNTs [Fig. 3(a)]. The Li-C bond length differences (0.03 and -0.03 Å) in the (4, 4) and (7, 0) CNTs are closest to zero among the studied CNTs, indicating similar chemical environments of Li ions at SS and TS.

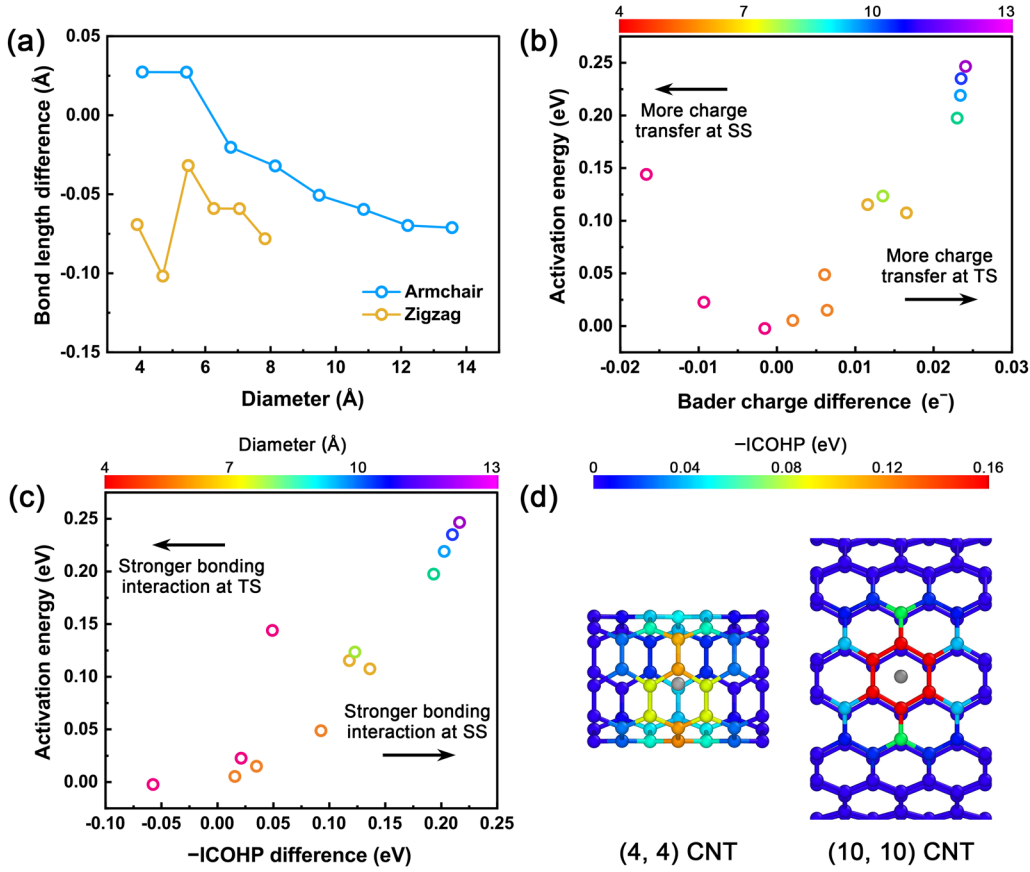


FIG. 3. The structural and electronic origin of Li-ion diffusions in CNTs. (a) Li-C bond length difference as a function of the diameter of CNTs. Activation energy as functions of (b) Li-ion Bader charge difference and (c) Li-C-ICOHP difference. (d) Li-C-ICOHP map of (4, 4) and (10, 10) CNTs with a Li atom.

The electron transfer between Li and CNTs is quantitatively revealed by Bader charges analysis. The largest Li Bader charge of $0.89 e^-$ is received in the (4, 4) and (7, 0) CNTs (Fig. S5). The (3, 3), (4, 4), and (7, 0) CNTs with low activation energies show small differences between Li Bader charges at SS and TS [Fig. 3(b)]. Such a correlation highlights the significance of a similar chemical environment of the Li ion on the low activation energy. A similar correlation was reported to explain the defect-facilitating Li diffusion across graphene and h-BN.⁴²

COHP is a theoretical analysis tool for bonding chemistry, which reveals the bonding and antibonding contribution to the electronic band energy. An energy integral of the COHP (ICOHP) determines the contribution of a chemical bond to the band energy, i.e., an indicator of bond strength. The ICOHPs of all Li-C pairs within a distance of 4 \AA are summed to evaluate the bonding interaction between the Li ion and CNT. The total -ICOHPs decrease with increasing diameters of CNTs (Fig. S6). The differences between total -ICOHPs at SS and TS are close to zero for the CNTs with low activation energy [Fig. 3(c)], verifying the significance of a similar chemical environment on the fast Li-ion transport again. The Li ion bonds with the nearest C ring in a large-diameter CNT, compared to the homogeneous bonding between Li and multiple C rings in a small-diameter CNT [Fig. 3(d)]. The decreasing number of bonding C rings is responsible for the decreasing -ICOHPs with increasing diameters of CNTs.

C. Li-ion transport at high carrier concentration

It is speculated that CNTs can serve as fast Li-ion transport channels based on the above energetical analysis. A high carrier concentration is indispensable for a high ionic conductivity besides low activation energy, which has been demonstrated as the origin of fast interfacial Li-ion transport in solid electrolyte interphases.⁴³ Therefore, the effect of carrier concentration on the Li-ion transport in CNTs is discussed. A closely packed configuration of CNT arrays is modeled to estimate the carrier (i.e., Li ion) concentration (Fig. S7). Carrier concentrations ranging from 1.7 to 10.5 mol L^{-1} are considered in this work [Fig. 4(a)]. Ten independent AIMD simulations are performed for the CNT with a preset carrier concentration. Diffusivities and ionic conductivities decrease with increasing carrier concentrations in the (4, 4) and (7, 0) CNTs [Figs. 4(b) and S8(a)]. Note that CNTs are widely used for anode materials.^{22–24} The Li-ion transports in CNTs with high carrier (i.e., Li ion) concentrations are realistic based on a consideration of practical applications. Diffusivities of 6.1×10^{-8} and $9.9 \times 10^{-8} \text{ m}^2 \text{ s}^{-1}$ and ionic conductivities of 19.9 and 29.5 S cm^{-1} are predicted in the (4, 4) and (7, 0) CNTs with carrier concentrations of 8.5 and 8.0 mol L^{-1} , respectively. The diffusivities are higher than the routine electrode materials (Fig. S9), which is expected to guarantee a fast Li-ion chemical diffusion driven by a concentration gradient. The ionic conductivities are significantly higher than the routine SE materials (Fig. S10). Note

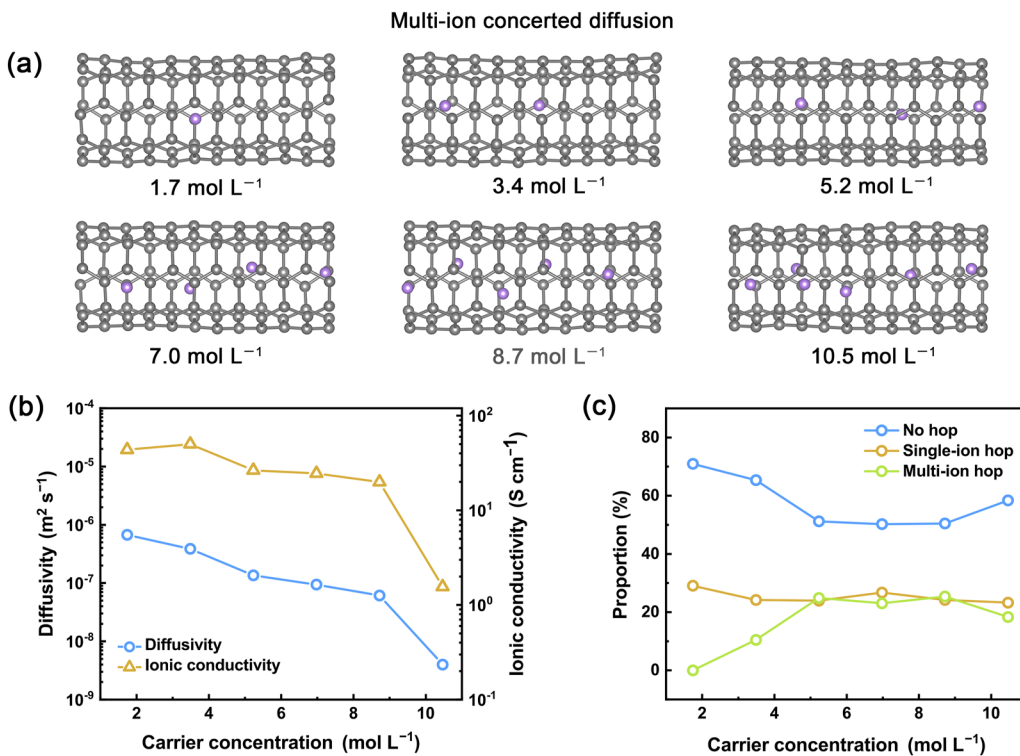


FIG. 4. The multi-ion concerted diffusion in CNTs. (a) The snapshots of the Li-ion distributions in the (4, 4) CNT with different carrier concentrations. The C and Li atoms are marked gray and pink, respectively. (b) Diffusivity and ionic conductivity and (c) the proportion of different ion hop states as a function of carrier concentration in the (4, 4) CNT.

that the theoretical prediction value is five orders of magnitude larger than the experimental value regarding the Li-ion transport in CNTs. The difference is attributed to two aspects. (1) The diameter of experimentally used CNTs is about 100 nm,²² much larger than the optimal predicted value. A large improvement in the ionic conductivity is expected by the controlled synthesis of CNTs. (2) A real CNT material exhibits a porosity of more than 90%,⁴⁴ implying a possible tenfold overestimation of predicted ionic conductivities. However, an ionic conductivity up to 10^{-1} – 10^0 S cm⁻¹ order of magnitudes is still fascinating for potential ion-conducting applications.

To quantitatively understand the multi-Li-ion diffusions in CNTs, A function $h_i(t; a, t_a)$ is defined to identify explicit Li-ion displacements,^{45–47}

$$h_i(t; a, \Delta t) = \theta\left(\left|r_i\left(t + \frac{\Delta t}{2}\right) - r_i\left(t - \frac{\Delta t}{2}\right)\right| - a\right), \quad (6)$$

where θ is the Heaviside step function. The difference $r_i\left(t + \frac{\Delta t}{2}\right) - r_i\left(t - \frac{\Delta t}{2}\right)$ describes the displacement of atom i . The displacement threshold a was set to 2 Å. The proportion of no hop, single hop, and multi-ion hop in the (4, 4) and (7, 0) CNTs are counted based on the Li-ion displacements (Figs. S11 and S12). The increasing proportion of multi-ion hop with an increasing carrier concentration indicates the concerted diffusion in the CNTs with high carrier concentrations [Figs. 4(c) and S8(b)]. Such evidence indicates the contribution of concerted diffusion to high ionic conductivities of CNTs,⁴⁸ similar to those in routine SEs.^{16,49}

The (3, 3), (4, 4), and (7, 0) CNTs with small diameters are usually grown inside thicker CNTs as inner tubes in double-walled CNTs (DWCNTs) rather than freestanding single-walled CNTs.⁵⁰ The Li-ion diffusions in DWCNTs are simulated for comparison. Slightly increased activation energies are obtained in the DWCNTs composed of (3, 3)/(4, 4) CNTs compared with those of the free-standing counterparts (Fig. S13), providing a promising approach for the practical ion-conducting application of CNTs.

The fast Li-ion transport in CNTs is of fundamental interest in several aspects, including the potential ion-conducting application of CNTs, the understanding of Li-ion transport in solids, and the rational design of high-ionic-conductivity solid materials. First, Li ions can enter the CNTs through the end of the CNTs or the topological defects.^{39,41} The nanochannel inside the CNTs provides a unique and fast ion-conducting pathway to avoid the possible effect of the complex environment on Li-ion transport. Second, several descriptors, including bond length, electron transfer, and bonding interaction are proposed to establish the correlation between structures and the transport properties of Li ions. Similar chemical environments of Li ions during their diffusions are a prerequisite for solid materials with fast Li-ion transports. Third, high-throughput material screening and big data research assisted by artificial intelligence can be performed based on these descriptors of transport properties, which are expected to accelerate material design and rationalize the design of high-ionic-conductivity solid materials.

IV. CONCLUSIONS

In conclusion, the Li-ion transport mechanism in CNTs is systematically probed. The armchair- and zigzag-type CNTs with a

diameter of 5.5 Å are predicted to exhibit an extremely low Li-ion diffusion barrier of about 10 meV, demonstrating a primary influence of diameter on ionic transport compared with that of chirality. The detailed structural and electronic structure analyses indicate that the ultralow diffusion barrier is attributed to similar chemical environments for Li ions during Li-ion diffusions. The concerted diffusion of Li ions ensures an ultrahigh ionic conductivity (19.9 and 29.5 S cm⁻¹) of the CNTs with a high carrier concentration of 8 mol L⁻¹. These results help broaden the outlook for the practical ion-conducting applications of CNTs and provide a new design idea for high-ionic-conductivity solid materials.

SUPPLEMENTARY MATERIAL

See the [supplementary material](#) for the energy profile of Li-ion diffusions, structural and electronic structure analyses, the time evolution of Li displacement events, and the activation energies of SWCNT and DWCNT.

ACKNOWLEDGMENTS

This work was supported by the National Key Research and Development Program (Grant No. 2021YFB2500300), Beijing Municipal Natural Science Foundation (Grant No. Z200011), National Natural Science Foundation of China (Grant Nos. 22109086, U1801257, 21825501, and 22209094), China Postdoctoral Science Foundation (Grant Nos. 2021TQ0161 and 2021M691709), and Grant No. 2020GQG1006 from the Guoqiang Institute at Tsinghua University. The authors acknowledged the support from Tsinghua National Laboratory for Information Science and Technology for theoretical simulations. X. Chen appreciates the support from the Shuimu Tsinghua Scholar Program of Tsinghua University and the Young Elite Scientists Sponsorship Program by CAST. We thank Dr. Xia-Xia Ma and Shu-Hao Wang for helpful discussions.

AUTHOR DECLARATIONS

Conflict of Interest

The authors have no conflicts to disclose.

Author Contributions

Zhong-Heng Fu: Data curation (equal); Formal analysis (equal); Investigation (equal); Writing – original draft (equal). **Xiang Chen:** Conceptualization (equal); Funding acquisition (equal); Project administration (equal); Resources (equal); Writing – original draft (equal); Writing – review & editing (equal). **Nan Yao:** Methodology (equal); Writing – review & editing (equal). **Le-Geng Yu:** Methodology (equal); Writing – review & editing (equal). **Xin Shen:** Methodology (equal); Writing – review & editing (equal). **Shaochen Shi:** Methodology (equal); Writing – review & editing (equal). **Rui Zhang:** Methodology (equal); Writing – review & editing (equal). **Zhengju Sha:** Methodology (equal); Writing – review & editing (equal). **Shuai Feng:** Methodology (equal); Writing – review & editing (equal). **Yu Xia:** Methodology (equal); Writing – review & editing (equal). **Qiang Zhang:** Conceptualization (equal); Funding acquisition (equal); Project administration (equal);

Resources (equal); Supervision (equal); Writing – review & editing (equal).

DATA AVAILABILITY

The data that support the findings of this study are available from the corresponding author upon reasonable request.

REFERENCES

- ¹Z.-H. Fu, X. Chen, and Q. Zhang, “Review on the lithium transport mechanism in solid-state battery materials,” *Wiley Interdiscip. Rev.: Comput. Mol. Sci.* e1621 (published online 2022).
- ²R. M. Ormerod, “Solid oxide fuel cells,” *Chem. Soc. Rev.* **32**, 17 (2003).
- ³H. Yuan, L. Kong, T. Li, and Q. Zhang, “A review of transition metal chalcogenide/graphene nanocomposites for energy storage and conversion,” *Chin. Chem. Lett.* **28**, 2180 (2017).
- ⁴T. Famprakis, P. Canepa, J. A. Dawson, M. S. Islam, and C. Masquelier, “Fundamentals of inorganic solid-state electrolytes for batteries,” *Nat. Mater.* **18**, 1278 (2019).
- ⁵X.-B. Cheng, C.-Z. Zhao, Y.-X. Yao, H. Liu, and Q. Zhang, “Recent advances in energy chemistry between solid-state electrolyte and safe lithium-metal anodes,” *Chem* **5**, 74 (2019).
- ⁶R. Murugan, V. Thangadurai, and W. Weppner, “Fast lithium ion conduction in garnet-type $\text{Li}_2\text{La}_3\text{Zr}_2\text{O}_{12}$,” *Angew. Chem., Int. Ed.* **46**, 7778 (2007).
- ⁷A. Martínez-Juárez, C. Pecharromán, J. E. Iglesias, and J. M. Rojo, “Relationship between activation energy and bottleneck size for Li^+ ion conduction in NASICON materials of composition $\text{LiMM}'(\text{PO}_4)_3$; M, M' = Ge, Ti, Sn, Hf,” *J. Phys. Chem. B* **102**, 372 (1998).
- ⁸Y. Inaguma, L. Chen, M. Itoh, and T. Nakamura, “Candidate compounds with perovskite structure for high lithium ionic conductivity,” *Solid State Ionics* **70–71**, 196 (1994).
- ⁹N. Kamaya, K. Homma, Y. Yamakawa, M. Hirayama, R. Kanno, M. Yonemura, T. Kamiyama, Y. Kato, S. Hama, K. Kawamoto, and A. Mitsui, “A lithium superionic conductor,” *Nat. Mater.* **10**, 682 (2011).
- ¹⁰H.-J. Deiseroth, S.-T. Kong, H. Eckert, J. Vannahme, C. Reiner, T. Zaif, and M. Schlosser, “ $\text{Li}_6\text{PS}_5\text{X}$: A class of crystalline Li-rich solids with an unusually high Li^+ mobility,” *Angew. Chem., Int. Ed.* **47**, 755 (2008).
- ¹¹M. B. Ley, S. Boulineau, R. Janot, Y. Filinchuk, and T. R. Jensen, “New Li ion conductors and solid state hydrogen storage materials: $\text{LiM}(\text{BH}_4)_3\text{Cl}$, M = La, Gd,” *J. Phys. Chem. C* **116**, 21267 (2012).
- ¹²T. Lapp, S. Skaarup, and A. Hooper, “Ionic conductivity of pure and doped Li_3N ,” *Solid State Ionics* **11**, 97 (1983).
- ¹³M. Matsuo and S.-i. Oriimo, “Lithium fast-ionic conduction in complex hydrides: Review and prospects,” *Adv. Energy Mater.* **1**, 161 (2011).
- ¹⁴H. D. Lutz, P. Kuske, and K. Wussow, “Ionic motion of tetrahedrally and octahedrally coordinated lithium ions in ternary and quaternary halides,” *Solid State Ionics* **28–30**, 1282 (1988).
- ¹⁵Y. Zhang, X. He, Z. Chen, Q. Bai, A. M. Nolan, C. A. Roberts, D. Banerjee, T. Matsunaga, Y. Mo, and C. Ling, “Unsupervised discovery of solid-state lithium ion conductors,” *Nat. Commun.* **10**, 5260 (2019).
- ¹⁶X. He, Y. Zhu, and Y. Mo, “Origin of fast ion diffusion in super-ionic conductors,” *Nat. Commun.* **8**, 15893 (2017).
- ¹⁷W. Xu, X. Pei, C. S. Diercks, H. Lyu, Z. Ji, and O. M. Yaghi, “A metal–organic framework of organic vertices and polyoxometalate linkers as a solid-state electrolyte,” *J. Am. Chem. Soc.* **141**, 17522 (2019).
- ¹⁸J. R. Sanchez-Valencia, T. Dienel, O. Gröning, I. Shorubalko, A. Mueller, M. Jansen, K. Amsharov, P. Ruffieux, and R. Fasel, “Controlled synthesis of single-chirality carbon nanotubes,” *Nature* **512**, 61 (2014).
- ¹⁹M. Ouyang, J.-L. Huang, C. L. Cheung, and C. M. Lieber, “Energy gaps in ‘metallic’ single-walled carbon nanotubes,” *Science* **292**, 702 (2001).
- ²⁰G. Hummer, J. C. Rasaiah, and J. P. Noworyta, “Water conduction through the hydrophobic channel of a carbon nanotube,” *Nature* **414**, 188 (2001).
- ²¹W. Choi, Z. W. Ulissi, S. F. E. Shimizu, D. O. Bellisario, M. D. Ellison, and M. S. Strano, “Diameter-dependent ion transport through the interior of isolated single-walled carbon nanotubes,” *Nat. Commun.* **4**, 2397 (2013).
- ²²Y. Chen, Z. Wang, X. Li, X. Yao, C. Wang, Y. Li, W. Xue, D. Yu, S. Y. Kim, F. Yang, A. Kushima, G. Zhang, H. Huang, N. Wu, Y.-W. Mai, J. B. Goodenough, and J. Li, “Li metal deposition and stripping in a solid-state battery via Coble creep,” *Nature* **578**, 251 (2020).
- ²³T. Fuchs, C. G. Haslam, A. C. Moy, C. Lerch, T. Krauskopf, J. Sakamoto, F. H. Richter, and J. Janek, “Increasing the pressure-free stripping capacity of the lithium metal anode in solid-state-batteries by carbon nanotubes,” *Adv. Energy Mater.* **12**, 2201125 (2022).
- ²⁴P. Wei, Y. Cheng, X. Yan, W. Ye, X. Lan, L. Wang, J. Sun, Z. Yu, G. Luo, Y. Yang, M. H. Rummeli, and M.-S. Wang, “Mechanistic probing of encapsulation and confined growth of lithium crystals in carbonaceous nanotubes,” *Adv. Mater.* **33**, 2105228 (2021).
- ²⁵G. Kresse and J. Furthmüller, “Efficient iterative schemes for *ab initio* total-energy calculations using a plane-wave basis set,” *Phys. Rev. B* **54**, 11169 (1996).
- ²⁶P. E. Blöchl, “Projector augmented-wave method,” *Phys. Rev. B* **50**, 17953 (1994).
- ²⁷D. M. Ceperley and B. J. Alder, “Ground state of the electron gas by a stochastic method,” *Phys. Rev. Lett.* **45**, 566 (1980).
- ²⁸T. Björkman, A. Gulans, A. V. Krasheninnikov, and R. M. Nieminen, “Are we van der Waals ready?,” *J. Phys.: Condens. Matter* **24**, 424218 (2012).
- ²⁹I. Hamada, “van der Waals density functional made accurate,” *Phys. Rev. B* **89**, 121103 (2014).
- ³⁰G. Henkelman, B. P. Uberuaga, and H. Jónsson, “A climbing image nudged elastic band method for finding saddle points and minimum energy paths,” *J. Chem. Phys.* **113**, 9901 (2000).
- ³¹Y. Liu, V. I. Artyukhov, M. Liu, A. R. Harutyunyan, and B. I. Yakobson, “Feasibility of lithium storage on graphene and its derivatives,” *J. Phys. Chem. Lett.* **4**, 1737 (2013).
- ³²G. Henkelman, A. Arnaldsson, and H. Jónsson, “A fast and robust algorithm for Bader decomposition of charge density,” *Comput. Mater. Sci.* **36**, 354 (2006).
- ³³R. Dranskiowski and P. E. Bloechl, “Crystal orbital Hamilton populations (COHP): Energy-resolved visualization of chemical bonding in solids based on density-functional calculations,” *J. Chem. Phys.* **97**, 8617 (1993).
- ³⁴S. Nosé, “A unified formulation of the constant temperature molecular dynamics methods,” *J. Chem. Phys.* **81**, 511 (1984).
- ³⁵W. G. Hoover, “Canonical dynamics: Equilibrium phase-space distributions,” *Phys. Rev. A* **31**, 1695 (1985).
- ³⁶Y. Gao, A. M. Nolan, P. Du, Y. Wu, C. Yang, Q. Chen, Y. Mo, and S.-H. Bo, “Classical and emerging characterization techniques for investigation of ion transport mechanisms in crystalline fast ionic conductors,” *Chem. Rev.* **120**, 5954 (2020).
- ³⁷N. Yao, X. Chen, Z.-H. Fu, and Q. Zhang, “Applying classical, *ab initio*, and machine-learning molecular dynamics simulations to the liquid electrolyte for rechargeable batteries,” *Chem. Rev.* **122**, 10970 (2022).
- ³⁸J. Yang, H. J. Liu, and C. T. Chan, “Theoretical study of alkali-atom insertion into small-radius carbon nanotubes to form single-atom chains,” *Phys. Rev. B* **64**, 085420 (2001).
- ³⁹V. Meunier, J. Kephart, C. Roland, and J. Bernholc, “*Ab initio* investigations of lithium diffusion in carbon nanotube systems,” *Phys. Rev. Lett.* **88**, 075506 (2002).
- ⁴⁰M. Zhao, Y. Xia, and L. Mei, “Diffusion and condensation of lithium atoms in single-walled carbon nanotubes,” *Phys. Rev. B* **71**, 165413 (2005).
- ⁴¹B. Song, J. Yang, J. Zhao, and H. Fang, “Intercalation and diffusion of lithium ions in a carbon nanotube bundle by *ab initio* molecular dynamics simulations,” *Energy Environ. Sci.* **4**, 1379 (2011).
- ⁴²H. Tian, Z. W. Seh, K. Yan, Z. Fu, P. Tang, Y. Lu, R. Zhang, D. Legut, Y. Cui, and Q. Zhang, “Theoretical investigation of 2D layered materials as protective films for lithium and sodium metal anodes,” *Adv. Energy Mater.* **7**, 1602528 (2017).

- ⁴³X.-X. Ma, X. Shen, X. Chen, Z.-H. Fu, N. Yao, R. Zhang, and Q. Zhang, "The origin of fast lithium-ion transport in the inorganic solid electrolyte interphase on lithium metal anodes," *Small Struct.* **3**, 2200071 (2022).
- ⁴⁴L. Dumee, L. Velleman, K. Sears, M. Hill, J. Schutz, N. Finn, M. Duke, and S. Gray, "Control of porosity and pore size of metal reinforced carbon nanotube membranes," *Membranes* **1**, 25 (2011).
- ⁴⁵M. Burbano, D. Carlier, F. Boucher, B. J. Morgan, and M. Salanne, "Sparse cyclic excitations explain the low ionic conductivity of stoichiometric Li₇La₃Zr₂O₁₂," *Phys. Rev. Lett.* **116**, 135901 (2016).
- ⁴⁶J. G. Smith and D. J. Siegel, "Low-temperature paddlewheel effect in glassy solid electrolytes," *Nat. Commun.* **11**, 1483 (2020).
- ⁴⁷H. Fang and P. Jena, "Argyrodite-type advanced lithium conductors and transport mechanisms beyond paddle-wheel effect," *Nat. Commun.* **13**, 2078 (2022).
- ⁴⁸M. Khantha, N. A. Cordero, J. A. Alonso, M. Cawkwell, and L. A. Girifalco, "Interaction and concerted diffusion of lithium in a (5, 5) carbon nanotube," *Phys. Rev. B* **78**, 115430 (2008).
- ⁴⁹Z.-H. Fu, X. Chen, N. Yao, X. Shen, X.-X. Ma, S. Feng, S. Wang, R. Zhang, L. Zhang, and Q. Zhang, "The chemical origin of temperature-dependent lithium-ion concerted diffusion in sulfide solid electrolyte Li₁₀GeP₂S₁₂," *J. Energy Chem.* **70**, 59 (2022).
- ⁵⁰L. Guan, K. Suenaga, and S. Iijima, "Smallest carbon nanotube assigned with atomic resolution accuracy," *Nano Lett.* **8**, 459 (2008).